Research Square

Preprints are preliminary reports that have not undergone peer review.
They should not be considered conclusive, used to inform clinical practice,
or referenced by the media as validated information.

Shared Brain Structural Correlates of Gait Abnormalities and Clinical Phenotypes in Multiple System Atrophy Cerebellar Type

Maolin Cui
Department of Rehabilitation Medicine, The First Affiliated Hospital of Fujian Medical University

xia liu
Department of Rehabilitation Medicine, Yantai Hospital Affiliated to Shandong Medical University, Yantai, China.

yue zhang
College of Mechanical Engineering and Automation, Fuzhou University

zhuo-ying huang
Department of Neurology, Fujian Institute of Neurology, The First Affiliated Hospital of Fujian Medical University

chu-yi li
Department of Neurology, Fujian Institute of Neurology, The First Affiliated Hospital of Fujian Medical University

wei Lin
Department of Neurology, Fujian Institute of Neurology, The First Affiliated Hospital of Fujian Medical University

bei-ning Ye
Department of Neurology, Fujian Institute of Neurology, The First Affiliated Hospital of Fujian Medical University

zhi-ye huang
Department of Neurology, Fujian Institute of Neurology, The First Affiliated Hospital of Fujian Medical University

si-min Wang
Department of Neurology, Fujian Institute of Neurology, The First Affiliated Hospital of Fujian Medical University

han lin
Department of Neurology, Fujian Institute of Neurology, The First Affiliated Hospital of Fujian Medical University

shi-rui Gan
ganshirui@fjmu.edu.cn

Department of Radiology, The First Affiliated Hospital of Fujian Medical University

Jian-Ping Hu

Department of Radiology, The First Affiliated Hospital of Fujian Medical University

Xin-Yuan chen

Clinical Center of Neuroregulation and Brain-Computer Interface, National Regional Medical Center, Binhai Campus

jun ni

Department of Rehabilitation Medicine, The First Affiliated Hospital of Fujian Medical University

---

Research Article

Keywords: multiple system atrophy, gait, digital biomarkers, disease severity, structural magnetic resonance imaging

Posted Date: November 27th, 2026

DOI: https://doi.org/10.21203/rs.3.rs-11812953/v1

License: This work is licensed under a Creative Commons Attribution 4.0 International License. Read Full License

Additional Declarations: No competing interests reported.

Abstract

Background

Gait impairment is prominent in multiple system atrophy of the cerebellar type (MSA-C), but the clinical correlates of individual gait abnormalities, their shared brain structural correlates, and their potential as clinically interpretable markers remain unclear.

Objectives

To identify convergent regional and whole-map gray-matter patterns between gait abnormalities and clinical phenotypes, and to prioritize clinically interpretable gait markers.

Methods

Thirty-nine patients with MSA-C and 36 healthy controls underwent smart-insole assessment of 20 gait features spanning pace, rhythm, support control, and angular control. Age-adjusted group comparisons were followed by age- and sex-adjusted clinical correlations. In 36 patients, regional overlap, whole-map spatial correspondence, and rank-rank hypergeometric overlap were used to assess structural convergence between gait features and clinical phenotypes. Gait markers were prioritized by cross-validation and bootstrap resampling.

Results

Twelve of 20 gait features differed between groups after BH-FDR correction ($q < 0.05$), with phenotype-specific gait-domain associations. Whole-map correspondence was positive for all 10 phenotype-gait pairs (nominal permutation $P < 0.05$ in seven) and strongest for UMSARS-II with stride length ($r_{map} = 0.648$), with regional overlap in vermal lobules VI–VIII, left locus coeruleus, right cerebellar lobule IX, and right ventromedial prefrontal cortex. SARA corresponded most strongly with cadence CV, and disease duration and age at onset with toe-off angle. Stride length and toe-off angle ranked highest for UMSARS-II and disease duration.

Conclusions

MSA-C gait impairment is multidimensional, and clinical phenotypes and associated gait abnormalities show partially convergent gray-matter correlates. Stride length and toe-off angle are interpretable candidate markers of motor severity and disease duration pending longitudinal validation.

Introduction

Gait impairment is common across neurodegenerative disorders [1–3], occurring in monogenic conditions such as Huntington's disease and spinocerebellar ataxias as well as in Alzheimer's disease and Parkinson's disease [4–7]. It increases the risk of falls, limits mobility and independence, reduces quality of life, and is associated with decreased survival [8, 9]. Quantitative gait measures are therefore increasingly used as digital markers of disease burden and progression [10, 11].

Multiple system atrophy of the cerebellar type (MSA-C) is an aggressive α-synucleinopathy marked by progressive gait ataxia, postural instability, and autonomic dysfunction, and gait impairment is among its most disabling manifestations [12, 13]. Quantitative gait measures have accordingly been proposed as digital biomarkers in MSA-C and related ataxias [14–16]. The study closest to the present work derived a composite gait-pattern score from two-dimensional video and showed that it correlated with motor severity, global cognitive scores, and cerebellar and middle temporal gray-matter volume [15]. A composite score, however, cannot show which gait dimension carries which clinical information, and that study related the gait score and motor severity to brain structure separately. Whether a gait measure and the clinical phenotype it tracks relate to the same brain regions therefore remains untested.

Gait features need not reflect a single underlying process. Pace, rhythm, support control, and angular control depend on overlapping but nonidentical components of locomotor regulation, and the clinical picture of MSA-C likewise spans motor severity, disease duration, age at onset, and cognitive function [17–19]. Defining which gait dimension corresponds to which clinical phenotype may therefore be more informative than treating gait as a unitary composite.

Such correspondences are more convincing if they are also anatomically grounded. Gait control depends on coordinated activity across brainstem, cerebellar, thalamic, basal-ganglia, and distributed cortical systems [20, 21], and different gait domains map onto partially distinct structural patterns [22, 23]. If a gait feature tracks a clinical phenotype because both index the same regional degeneration, their gray-matter correlates should coincide, both in thresholded regions and across the whole pattern of regional effects. Such convergence would support the gait feature as a biologically plausible proxy for that phenotype; its absence would indicate a behavioral association without a common structural basis.

For clinical use, a marker should also be simple: a single gait measure in its native unit is easier to interpret and follow than a multivariable model. We therefore (1) characterized age-adjusted abnormalities across 20 spatiotemporal gait features and their associations with motor severity, disease duration, age at onset, and cognition; (2) tested whether clinically linked gait features and clinical phenotypes share regional and whole-map gray-matter correlates; and (3) ranked single gait measures as candidate markers of motor severity and disease duration. We hypothesized that different clinical phenotypes would be associated with different gait domains, and that the structural-effect map of each phenotype would correlate positively with the maps of its associated gait features.

Methods

Study Participants and Clinical Assessment

This study was conducted in accordance with the Declaration of Helsinki and reported following the STROBE guidelines. The protocol and informed-consent procedures were approved by the Ethics Committee of the First Affiliated Hospital of Fujian Medical University (MRCTA, ECFAH of FMU [2022] 399). Participants were recruited through the Chinese Southeast Spinocerebellar Ataxia Research Organization (OSCCAR) at the Department of Neurology, First Affiliated Hospital of Fujian Medical University (ClinicalTrials.gov identifier: NCT04010214), and all participants provided written informed consent.

We enrolled 39 patients with MSA-C and 36 healthy controls (HCs) from outpatient clinics and unaffected relatives. All patients met the 2022 Movement Disorder Society criteria for clinically established or clinically probable MSA-C [13]. Additional inclusion criteria were disease duration < 4 years, independent ambulation with or without an assistive device, anticipated survival > 3 years, and effective contraception in women of childbearing potential. Exclusion criteria included other neurological disorders, marked cognitive-behavioral deficits or psychiatric illness, severe systemic disease, recent head injury or neurosurgery, recent investigational treatment, pregnancy or breastfeeding, and MRI contraindications. Structural analyses were restricted to the 36 patients with complete MRI, gait, and clinical data.

Demographic and clinical information was collected by an independent neurologist. Age at onset was defined as the age at which the patient or family first noticed ataxic symptoms, and disease duration was calculated from symptom onset to study assessment. Motor impairment was evaluated using the Scale for the Assessment and Rating of Ataxia (SARA) [24] and the Unified Multiple System Atrophy Rating Scale (UMSARS) [25], with UMSARS-II prespecified as the principal motor examination measure. Cognitive performance was assessed using the Mini-Mental State Examination (MMSE) [26] and Montreal Cognitive Assessment (MoCA) [27].

Smart-Insole Gait Assessment

Gait was assessed using a wearable smart-insole system integrating plantar-pressure sensing and inertial measurement. Pressure and inertial signals were calibrated before testing, synchronized using a common timestamp, and recorded in real time. The platform and sensor technology have been described previously [28, 29]; additional acquisition and feature-derivation details are provided in Supplementary Methods S1.

Twenty spatiotemporal gait features were analyzed: gait velocity, stride length, cadence, cadence SD, cadence coefficient of variation (CV), stride time, stride time SD, stride time CV, single-support percentage, single-support SD, single-support CV, double-support percentage, double-support SD, double-support CV, toe-out angle, toe-out angle SD, toe-out angle CV, toe-off angle, toe-off angle SD, and toe-off angle CV. CV was calculated as SD divided by the corresponding mean and multiplied by 100. For clinical

interpretation, the features were organized into four biomechanical domains: pace, rhythm, support control, and angular control.

MRI Acquisition and Structural Analysis

Structural MRI was acquired on a 3.0-T Siemens Skyra scanner using a sagittal T1-weighted MP-RAGE sequence (TR = 2300 ms, TE = 2.3 ms, TI = 900 ms, flip angle = 8°, field of view = 240×256 mm^2, matrix = 240×256, bandwidth = 200 Hz/Px, 192 slices, isotropic voxel size = 1×1×1 mm^3; acquisition time 5 min 12 s). T1-weighted images were processed in SPM12 with CAT12 [30]. Preprocessing comprised bias-field correction, tissue segmentation, DARTEL-based normalization to MNI space [31], Jacobian modulation to preserve regional volume information, and smoothing of gray-matter maps with an 8-mm full-width at half-maximum Gaussian kernel.

Regional gray-matter volume (GMV) was extracted using the Automated Anatomical Labeling Atlas 3 (AAL3) parcellation [32]. The regional table initially contained 170 variables; seven regions had zero between-subject variance and were excluded, leaving 163 analyzable ROIs in the 36-patient MRI sample (Supplementary Table S13). Additional preprocessing and regional-extraction details are provided in Supplementary Methods S3.

Clinical-Gait and Structural Convergence Analyses

Continuous variables were summarized as mean ± SD or median (Q1, Q3), according to distribution, and categorical variables as n (%). Baseline group characteristics were compared using independent-samples t tests or Mann-Whitney U tests for continuous variables and chi-square or Fisher exact tests for categorical variables, as appropriate. Because the HC group was younger than the MSA-C group, each of the 20 gait features was compared between groups using a general linear model with group as the predictor and age as a covariate. Benjamini-Hochberg false-discovery-rate (BH-FDR) correction [33] was applied across the 20 gait comparisons, and features with FDR-adjusted $P < 0.05$ were defined as abnormal. Within the MSA-C group, these abnormal features were then related to UMSARS-II, SARA, MoCA, disease duration, and age at onset using two-sided partial Pearson correlations adjusted for age and sex. Disease duration was available in 38 patients and the remaining clinical variables in 39. This clinical-gait screen was prespecified as the entry step for the exploratory structural analysis; nominal $P < 0.05$ was therefore used to identify phenotype-gait associations carried forward.

Representative gait features were selected before inspection of the MRI results. For each clinical phenotype, only gait domains containing at least one abnormal feature associated with that phenotype at nominal $P < 0.05$ were eligible. If more than one feature within a domain met this criterion, the feature with the largest absolute age- and sex-adjusted partial-correlation coefficient was selected, yielding 10 clinically defined phenotype-gait pairs. For each representative gait feature and each clinical phenotype, partial Pearson correlations were then calculated between regional GMV and the variable of interest

while adjusting for age, sex, and total intracranial volume. Nominal two-sided $P < 0.05$ was used for exploratory regional localization. A direct shared ROI was defined as the same AAL3 region meeting this threshold in both the clinical-phenotype map and its corresponding gait-feature map.

To evaluate convergence independently of the ROI-level significance threshold, all 163 regional partial-correlation coefficients were retained as complete structural-effect vectors. Directions were harmonized so that higher variable values consistently represented greater impairment; after harmonization, negative coefficients indicated lower GMV with greater impairment. For each of the 10 phenotype-gait pairs, whole-map spatial correspondence was quantified as the Spearman correlation between the two 163-ROI effect vectors (r_{map}) and assessed using a two-sided subject-level permutation test. For each pair, the clinical phenotype residuals after adjustment for age, sex, and total intracranial volume were permuted 10,000 times while the gait map was held fixed; the clinical structural-effect map and r_{map} were recalculated for each permutation. Nominal two-sided P values were calculated from the absolute null and observed r_{map} values. These exploratory P values were not adjusted for the 10 pairwise comparisons. The strongest common damage-oriented component was further localized using rank-rank hypergeometric overlap (RRHO) [34]. Negative-effect ROIs were ranked from strongest to weakest in each map, hypergeometric enrichment was evaluated across all combinations of clinical and gait rank thresholds in one-ROI increments, and the threshold pair with the smallest hypergeometric survival probability defined the RRHO peak and its shared ROI set. Because the peak was selected adaptively across multiple rank combinations, peak hypergeometric P values were treated as descriptive. For phenotypes represented by more than one gait dimension, pairwise RRHO sets were additionally classified as common-core, partially shared, or gait-dimension-specific regions and compared using Jaccard and Dice similarity. Implementation details and the complete RRHO landscapes are provided in Supplementary Methods S5 and Supplementary Figure S1.

Gait-Marker Prioritization and Statistical Analysis

Candidate markers for motor severity comprised abnormal gait features that were significantly associated with UMSARS-II in the clinical-gait screen; candidate markers for disease duration were defined analogously. Each candidate was evaluated in an age- and sex-adjusted single-marker model using repeated 5-fold cross-validation with 500 repeats. Within each outcome, held-out performance was normalized to the best-performing candidate, which was assigned a relative performance of 100%; these values were used for within-outcome ranking rather than interpreted as absolute predictive accuracy. Ranking stability was assessed with 10,000 patient-level bootstrap resamples, in each of which the candidate-performance framework was recomputed and reranked. Stability was summarized as the percentage of resamples in which each marker ranked first and the percentage in which it ranked among the top three.

For direct clinical interpretation of the leading markers, age- and sex-adjusted linear regression modeled UMSARS-II as a function of stride length expressed in centimeters and toe-off angle as a function of disease duration expressed in years. Unstandardized regression coefficients were reported in native

clinical units. Analyses were performed in R version 4.5.2 except for the permutation testing of whole-map correspondence, which was performed in Python using NumPy and SciPy. All reported tests were two sided, with multiplicity correction and nominal thresholds applied as described for each analytic stage above. Additional details of the marker-ranking and regression procedures are provided in Supplementary Methods S6.

Results

Baseline and Clinical Characteristics

Healthy controls were significantly younger than patients with MSA-C (42.92 ± 15.37 vs. 56.41 ± 7.57 years, P<0.001). Height, weight, and sex distribution did not differ significantly between groups (all P>0.05; Table 1). Within the MSA-C cohort, median disease duration was 2 years (Q1, Q3: 2, 3), median age at onset was 53 years (51, 58.5), mean SARA score was 12.33 ± 3.92, mean total UMSARS score was 27.18 ± 8.80, mean UMSARS-I score was 12.95 ± 4.44, and median UMSARS-II score was 14 (10, 16). Median MMSE score was 25 (22.5, 28), and mean MoCA score was 17.2 ± 6.51.

Gait Abnormalities and Their Clinical Correlates

Among the 20 spatiotemporal gait features, 12 differed significantly between patients with MSA-C and healthy controls after age adjustment and BH-FDR correction (Figure 1A; Supplementary Table S1). Compared with healthy controls, patients with MSA-C showed markedly reduced gait velocity (0.777 ± 0.179 vs. 1.097 ± 0.170 m/s, FDR-adjusted P<0.001) and stride length (0.435 ± 0.102 vs. 0.615 ± 0.086 m, FDR-adjusted P<0.001). Rhythm abnormalities were characterized by substantially greater cadence variability, including cadence SD (37.19 ± 3.86 vs. 18.46 ± 4.19, FDR-adjusted P<0.001) and cadence CV (34.51 ± 0.77 vs. 17.40 ± 4.58, FDR-adjusted P<0.001). Support-control abnormalities included increased single-support percentage (64.36 ± 3.93% vs. 61.38 ± 2.72%, FDR-adjusted P=0.007) and greater double-support variability (SD: 7.84 ± 4.60 vs. 4.29 ± 1.77, FDR-adjusted P=0.001; CV: 25.71 ± 11.87 vs. 16.65 ± 6.88, FDR-adjusted P=0.002). Angular-control abnormalities included increased toe-out angle (26.78 ± 6.38° vs. 11.67 ± 7.76°, FDR-adjusted P<0.001), reduced toe-off angle (13.63 ± 9.08° vs. 27.08 ± 11.04°, FDR-adjusted P<0.001), and greater variability in toe-out and toe-off measures. Collectively, the abnormal features spanned pace, rhythm, support control, and angular control.

Age- and sex-adjusted partial correlations showed phenotype-specific patterns (Figure 1B; Supplementary Table S2). UMSARS-II showed the broadest association pattern, involving all four gait domains, with the strongest association for stride length (r=-0.537, P<0.001). SARA was associated with gait abnormalities across pace, rhythm, and support-control domains, with cadence CV showing the strongest association (r=0.398, P=0.015). Disease duration was associated with pace and angular-control abnormalities, with toe-off angle showing the strongest association (r=-0.481, P=0.003). Age at onset showed a more selective pattern confined to the angular-control domain; toe-off angle showed the strongest association (r=0.521, P<0.001). In contrast, none of the abnormal gait features was significantly associated with MoCA after adjustment for age and sex (all P>0.05). These associations

determined the representative gait features carried forward to structural analysis (Supplementary Table S3).

Shared Brain Structural Correlates of Gait Abnormalities and Clinical Phenotypes

To examine whether the observed clinical-gait associations were accompanied by shared gray-matter correlates, we analyzed regional GMV associations in the 36 patients with complete MRI, gait, and clinical data. At a nominal threshold of $P<0.05$, gait velocity, stride length, cadence SD, cadence CV, single support, double-support SD, toe-off angle, and toe-off angle CV were associated with 15, 29, 20, 6, 3, 11, 18, and 27 ROIs, respectively. The corresponding clinical maps involved 9 ROIs for UMSARS-II, 3 for SARA, and 15 each for disease duration and age at onset (Figure 2A; Supplementary Tables S4-S5).

Regional overlap was then examined between each clinical phenotype and its corresponding gait features (Figure 2B-C; Supplementary Table S6). For UMSARS-II, stride length shared six ROIs—vermal lobules VI-VIII, the left locus coeruleus, right cerebellar lobule IX, and right ventromedial prefrontal cortex—whereas cadence SD shared vermal lobules VI and VIII and toe-off angle CV shared the left locus coeruleus, right cerebellar lobule IX, and right ventromedial prefrontal cortex; single support showed no nominal overlap. For SARA, overlap was observed only with cadence CV, involving the right ventral posterolateral thalamus. For disease duration, gait velocity and toe-off angle each shared five ROIs: gait velocity overlapped with vermal lobule X, bilateral ventromedial prefrontal cortex, the left middle temporal pole, and left reuniens nucleus, whereas toe-off angle overlapped with vermal lobule X, bilateral ventromedial prefrontal cortex, the left middle temporal pole, and right medial pulvinar. For age at onset, toe-off angle shared vermal lobule X, the left ventromedial prefrontal cortex, bilateral middle temporal poles, and right medial pulvinar. Lower GMV accompanied greater impairment in 19 of the 27 pairwise overlaps (cerebellar, locus coeruleus, and ventromedial prefrontal regions), and larger GMV in the remaining eight (temporal-pole and thalamic regions).

Whole-map analyses showed that these clinical-gait relationships extended beyond thresholded ROI overlap (Figure 2D-E; Supplementary Table S7; Supplementary Figure S1); r_map was positive in all 10 pairs (range, 0.347–0.648). For UMSARS-II, the strongest spatial correspondence was observed with stride length (r_map=0.648), with 46 ROIs shared at the RRHO peak and a distribution dominated by cerebellar hemispheric and vermal regions together with prefrontal and striatal structures. For SARA, cadence CV showed the strongest correspondence (r_map=0.574), with 25 shared ROIs mainly distributed across cerebellar-vermal and prefrontal-subcortical regions. Disease duration showed the strongest correspondence with toe-off angle (r_map=0.613), involving 12 shared ROIs predominantly within cerebellar-vermal and ventromedial prefrontal regions. Age at onset also corresponded with toe-off angle (r_map=0.568), with 17 shared ROIs showing a predominantly cerebellar-vermal-prefrontal distribution. Seven of the 10 whole-map correspondences had nominal two-sided permutation $P<0.05$; these exploratory values were not adjusted for multiplicity (Figure 2D; Supplementary Table S7). Across phenotypes linked to multiple gait dimensions, RRHO sets contained both common-core regions and

dimension-specific extensions, with their complete membership and pairwise set similarity reported in Figure 2E and Supplementary Tables S8-S10.

Clinically Interpretable Gait Markers for Motor Severity and Disease Duration

Candidate gait measures identified in the preceding clinical-gait analysis were ranked using repeated 5-fold cross-validation and bootstrap resampling (Figure 3A-B; Supplementary Table S11). For UMSARS-II, stride length demonstrated the highest relative performance (100.0%), followed by gait velocity (79.7%), single support (72.5%), and toe-off angle CV (67.3%). Across 10,000 bootstrap resamples, stride length ranked first in 36.4% of iterations and among the top three in 82.7%, compared with 33.7% and 54.7% for single support. For disease duration, toe-off angle showed the highest relative performance (100.0%), followed by toe-out angle SD (74.9%); all remaining candidate measures had relative performance below 40%. Toe-off angle ranked first in 51.1% of bootstrap resamples and among the top three in 94.6%.

Age- and sex-adjusted regression analyses provided direct clinical interpretation of the selected markers (Figure 3C-D; Supplementary Table S12). Across patients, each 1-cm shorter stride length was associated with an estimated 0.32-point higher UMSARS-II score (unstandardized β=-0.317, $P<0.001$), and each additional year of disease duration with an estimated 3.33° lower toe-off angle (unstandardized β=-3.328, $P=0.003$).

Discussion

Using smart-insole gait assessment in MSA-C, we report three findings. Twelve of 20 spatiotemporal features were abnormal and, as hypothesized, different phenotypes were associated with different gait domains, ranging from all four for UMSARS-II to angular control alone for age at onset; no feature was significantly associated with MoCA. Also as hypothesized, the structural-effect maps of each phenotype and its associated gait features were positively correlated in all 10 pairs, nominally significantly in seven. Finally, stride length and toe-off angle were the highest-ranked single-feature candidates for UMSARS-II and disease duration, although their rankings were only moderately stable.

Earlier work established prominent gait impairment and variability in MSA and related ataxias [14–16, 35]; our results add that individual features carry different clinical information. The breadth of the UMSARS-II associations is expected, because the motor examination rates gait, posture, and limb function together [25]. SARA, an ataxia-specific scale, was most closely related to cadence variability, in keeping with irregular step timing as a core feature of cerebellar gait [16, 35, 36]. The angular-control findings were the least anticipated: a lower toe-off angle and a larger, more variable toe-out angle accompanied longer disease duration, whereas no angular measure was significantly related to SARA. A lower toe-off angle indicates a flatter foot at push-off and thus a less propulsive step. Foot-angle measures may capture cumulative adaptation that ataxia scales weight little, but this remains speculative.

The absence of significant MoCA associations contrasts with the correlation between a composite gait score and cognitive scores reported previously [15]. Several features showed weak associations in the expected direction (for example, double-support SD, r=-0.320, P = 0.054), so the discrepancy may reflect limited power for single features compared with a composite. Cohort characteristics may also contribute: patients with marked cognitive deficits were excluded, and most had primary education or less, which lowers MoCA scores independently of disease [27, 37]. The null result should therefore not be read as evidence that gait and cognition are unrelated in MSA-C [17–19].

The structural analyses suggest that these clinical-gait relationships are accompanied by shared gray-matter correlates, with three caveats. First, the regions of direct overlap are not equally interpretable. Cerebellar vermal and hemispheric regions overlapped for UMSARS-II, disease duration, and age at onset and formed most of the RRHO common core, consistent with the olivopontocerebellar degeneration that defines MSA-C [12, 13] and with cerebellar gray-matter correlates of gait reported previously [15]; ventromedial prefrontal overlap is in line with cortical contributions to gait [20–23]. In contrast, temporal-pole and thalamic overlap, including the only overlap for SARA, reflected larger volume with greater impairment, which degeneration does not readily explain. The locus coeruleus and individual thalamic nuclei are also small relative to the 8-mm smoothing kernel, and all regional effects were identified at an uncorrected threshold. Second, whole-map correspondence was positive in every pair but nominally significant in only seven, and the pairs were selected because the gait feature and the phenotype were correlated across patients. Some map similarity is therefore expected by construction, and the permutation test, which held the selected pairs fixed, does not remove this dependence. Third, gray-matter volume does not capture the pontine and middle-cerebellar-peduncle white-matter degeneration that is central to MSA-C [12, 13, 15]. We therefore regard the findings as evidence of partially convergent structural correlates, not as proof that any region mediates a given gait phenotype.

Stride length ranked first for UMSARS-II, but in only 36.4% of bootstrap resamples, close to single support (33.7%); toe-off angle led more clearly for disease duration (51.1%). These are leading candidates among correlated measures, not uniquely best markers. The native-unit estimates aid interpretation, but they describe differences between patients in a cohort restricted to less than 4 years of disease and cannot be read as within-patient rates of change. Whether these measures track progression requires longitudinal testing, as has been done for digital gait measures in degenerative ataxias and other movement disorders [10, 11, 35, 38–40]. If confirmed, a single insole-derived measure could complement rating scales in clinical follow-up.

Several further limitations should be noted. The design was cross-sectional and the sample modest, with 36 patients in the structural analyses. Clinical-gait correlations, ROI-wise localization, and whole-map permutation tests used nominal thresholds, and RRHO peak probabilities were descriptive because rank thresholds were selected adaptively. Healthy controls were on average 13 years younger than patients, so the linear age adjustment involved extrapolation. Gait measures were not adjusted for height, which influences stride length. Because age equals age at onset plus disease duration, the age-adjusted associations of these two phenotypes are near mirror images and represent one finding, not two. The

marker ranking is not externally validated prediction accuracy. Finally, without MSA-P or other ataxia groups, disease specificity is unknown, and replication in independent longitudinal cohorts is required.

In conclusion, gait impairment in MSA-C is not a unitary motor manifestation. Different gait dimensions relate to different clinical phenotypes, and clinically linked gait features and phenotypes show partially convergent gray-matter correlates centered on the cerebellum. Stride length and toe-off angle are interpretable candidate markers of motor severity and disease duration that now require longitudinal validation.

Declarations

Acknowledgments

The authors thank the patients, their families and caregivers, and all members who participated in this research.

Ethics approval

The study was conducted in accordance with the Declaration of Helsinki and was approved by the Ethics Committee of the First Affiliated Hospital of Fujian Medical University (MRCTA, ECFAH of FMU [2022] 399).

Consent to participate

All participants provided written informed consent.

Competing interests

The authors declare no conflicts of interest relevant to this work. All authors report no financial disclosures for the previous 12 months.

Funding

This work was supported by the National Natural Science Foundation of China (Grant Nos. 82371879 to S.-R.G. and 82402952 to X.-Y.C.) and the Joint Funds for the Innovation of Science and Technology, Fujian, China (Grant No. 2025Y9237 to S.-R.G.).

Data availability

The data supporting the findings of this study are not publicly available because they contain information that could compromise participant privacy, but they are available from the corresponding author, Shi-Rui Gan, upon reasonable request and subject to institutional and ethical restrictions.

Authors' contributions

(1) Research Project: A. Conception, B. Organization, C. Execution; (2) Statistical Analysis: A. Design, B. Execution, C. Review and Critique; (3) Manuscript Preparation: A. Writing of the First Draft, B. Review and Critique.

Mao-Lin Cui: 1C, 2B, 3A, 3B; Xia Liu: 2B, 3A, 3B; Yue Zhang: 3A, 3B; Chu-Yi Li: 2B, 3B; Zhuo-Ying Huang: 2B, 3B; Wei Lin: 1C, 2B, 3A, 3B; Bei-Ning Ye: 2B, 3B; Zhi-Ye Huang: 2B, 3B; Si-Min Wang: 2B, 3B; Han Lin: 2B, 3B; Shi-Rui Gan: 1A, 1B, 1C, 2A, 2B, 2C, 3A, 3B; Jian-Ping Hu: 1A, 1B, 2A, 2C, 3B; Xin-Yuan Chen: 1A, 1B, 2A, 2C, 3B; Jun Ni: 1A, 1B, 2A, 2C, 3B. All authors reviewed and approved the final manuscript and agree to be accountable for all aspects of the work.

References

1. Ali F, Padilla H, Blazek AM, Barnard L, Kaufman KR. Gait Analysis in Neurologic Disorders: Methodology, Applications, and Clinical Considerations. Neurology. 2025;105:e214154. https://doi.org/10.1212/wnl.0000000000214154.
2. Pieruccini-Faria F, Black SE, Masellis M, et al. Gait variability across neurodegenerative and cognitive disorders: Results from the Canadian Consortium of Neurodegeneration in Aging (CCNA) and the Gait and Brain Study. Alzheimers Dement. 2021;17:1317–28. https://doi.org/10.1002/alz.12298.
3. Cicirelli G, Impedovo D, Dentamaro V, Marani R, Pirlo G, D'Orazio TR. Human Gait Analysis in Neurodegenerative Diseases: A Review. IEEE J Biomed Health Inf. 2022;26:229–42. https://doi.org/10.1109/jbhi.2021.3092875.
4. Gaßner H, Jensen D, Marxreiter F, et al. Gait variability as digital biomarker of disease severity in Huntington's disease. J Neurol. 2020;267:1594–601. https://doi.org/10.1007/s00415-020-09725-3.
5. Coarelli G, Coutelier M, Durr A. Autosomal dominant cerebellar ataxias: new genes and progress towards treatments. Lancet Neurol. 2023;22:735–49. https://doi.org/10.1016/s1474-4422(23)00068-6.
6. Gilat M, Nonnekes J, Factor SA, et al. An updated definition of freezing of gait. Nat Rev Neurol. 2026;22:172–81. https://doi.org/10.1038/s41582-025-01179-3.
7. Montero-Odasso MM, Sarquis-Adamson Y, Speechley M, et al. Association of Dual-Task Gait With Incident Dementia in Mild Cognitive Impairment: Results From the Gait and Brain Study. JAMA Neurol. 2017;74:857–65. https://doi.org/10.1001/jamaneurol.2017.0643.
8. Nonnekes J, Goselink RJM, Růžička E, Fasano A, Nutt JG, Bloem BR. Neurological disorders of gait, balance and posture: a sign-based approach. Nat Rev Neurol. 2018;14:183–9. https://doi.org/10.1038/nrneurol.2017.178.
9. Mirelman A, Bonato P, Camicioli R, et al. Gait impairments in Parkinson's disease. Lancet Neurol. 2019;18:697–708. https://doi.org/10.1016/s1474-4422(19)30044-4.
10. Seemann J, Daghsen L, Cazier M, et al. Digital Gait Measures Capture 1-Year Progression in Early-Stage Spinocerebellar Ataxia Type 2. Mov Disord. 2024;39:788–97. https://doi.org/10.1002/mds.29757.

11. Mirelman A, Volkov J, Salomon A, et al. Digital Mobility Measures: A Window into Real-World Severity and Progression of Parkinson's Disease. Mov Disord. 2024;39:328–38. https://doi.org/10.1002/mds.29689.
12. Krismer F, Fanciulli A, Meissner WG, Coon EA, Wenning GK. Multiple system atrophy: advances in pathophysiology, diagnosis, and treatment. Lancet Neurol. 2024;23:1252–66. https://doi.org/10.1016/s1474-4422(24)00396-x.
13. Wenning GK, Stankovic I, Vignatelli L, et al. The Movement Disorder Society Criteria for the Diagnosis of Multiple System Atrophy. Mov Disord. 2022;37:1131–48. https://doi.org/10.1002/mds.29005.
14. Manohar R, Yang FX, Stephen CD, et al. At-home wearables and machine learning capture motor impairment and progression in adult ataxias. Brain. 2025;148:3623–34. https://doi.org/10.1093/brain/awaf154.
15. Lee S, Kim M, Choi KS, et al. Clinical and neuroimaging correlates of disease related gait patterns in patients with multiple system atrophy cerebellar type. Sci Rep. 2025;15:43754. https://doi.org/10.1038/s41598-025-26389-z.
16. Sidoroff V, Raccagni C, Kaindlstorfer C, et al. Characterization of gait variability in multiple system atrophy and Parkinson's disease. J Neurol. 2021;268:1770–9. https://doi.org/10.1007/s00415-020-10355-y.
17. Eschlböck S, et al. Cognition in multiple system atrophy: a single-center cohort study. Ann Clin Transl Neurol. 2020;7:219–28. https://doi.org/10.1002/acn3.50987.
18. Lazzeri G, et al. Cognitive and Autonomic Dysfunction in Multiple System Atrophy Type P and C: A Comparative Study. Front Neurol. 2022;13:912820. https://doi.org/10.3389/fneur.2022.912820.
19. Stankovic I, et al. Cognitive impairment in multiple system atrophy: a position statement by the Neuropsychology Task Force of the MDS Multiple System Atrophy (MODIMSA) study group. Mov Disord. 2014;29:857–67. https://doi.org/10.1002/mds.25880.
20. Arber S, Costa RM. Networking brainstem and basal ganglia circuits for movement. Nat Rev Neurosci. 2022;23:342–60. https://doi.org/10.1038/s41583-022-00581-w.
21. Takakusaki K. Functional Neuroanatomy for Posture and Gait Control. J Mov Disord. 2017;10:1–17. https://doi.org/10.14802/jmd.16062.
22. Maidan I, Mirelman A, Hausdorff JM, Stern Y, Habeck CG. Distinct cortical thickness patterns link disparate cerebral cortex regions to select mobility domains. Sci Rep. 2021;11:6600. https://doi.org/10.1038/s41598-021-85058-z.
23. Wilson J, Allcock L, Mc Ardle R, Taylor JP, Rochester L. The neural correlates of discrete gait characteristics in ageing: A structured review. Neurosci Biobehav Rev. 2019;100:344–69. https://doi.org/10.1016/j.neubiorev.2018.12.017.
24. Schmitz-Hübsch T, Tezenas du Montcel S, Baliko L, et al. Scale for the assessment and rating of ataxia: development of a new clinical scale. Neurology. 2006;66:1717–20. https://doi.org/10.1212/01.wnl.0000219042.60538.92.

25. Wenning GK, Tison F, Seppi K, et al. Development and validation of the Unified Multiple System Atrophy Rating Scale (UMSARS). Mov Disord. 2004;19:1391–402. https://doi.org/10.1002/mds.20255.
26. Folstein MF, Folstein SE, McHugh PR. Mini-mental state. A practical method for grading the cognitive state of patients for the clinician. J Psychiatr Res. 1975;12:189–98. https://doi.org/10.1016/0022-3956(75)90026-6.
27. Nasreddine ZS, Phillips NA, Bédirian V, et al. The Montreal Cognitive Assessment, MoCA: a brief screening tool for mild cognitive impairment. J Am Geriatr Soc. 2005;53:695–9. https://doi.org/10.1111/j.1532-5415.2005.53221.x.
28. Xiao Y, Luo K, Zhang Y, et al. Interpretable machine learning for differentiating SCA3 and MSA-C using gait and postural features from wearable sensors. J Neuroeng Rehabil. 2026;23:36. https://doi.org/10.1186/s12984-025-01843-1.
29. Li W, Jin X, Han X, et al. Synergy of Porous Structure and Microstructure in Piezoresistive Material for High-Performance and Flexible Pressure Sensors. ACS Appl Mater Interfaces. 2021;13:19211–20. https://doi.org/10.1021/acsami.0c22938.
30. Gaser C, Dahnke R, Thompson PM, Kurth F, Luders E. Alzheimer's Disease Neuroimaging Initiative. CAT: a computational anatomy toolbox for the analysis of structural MRI data. Gigascience. 2024;13:giae049. https://doi.org/10.1093/gigascience/giae049.
31. Ashburner J. A fast diffeomorphic image registration algorithm. NeuroImage. 2007;38:95–113. https://doi.org/10.1016/j.neuroimage.2007.07.007.
32. Rolls ET, Huang CC, Lin CP, Feng J, Joliot M. Automated anatomical labelling atlas 3. NeuroImage. 2020;206:116189. https://doi.org/10.1016/j.neuroimage.2019.116189.
33. Benjamini Y, Hochberg Y. Controlling the false discovery rate: a practical and powerful approach to multiple testing. J R Stat Soc Ser B Stat Methodol. 1995;57:289–300. https://doi.org/10.1111/j.2517-6161.1995.tb02031.x.
34. Plaisier SB, Taschereau R, Wong JA, Graeber TG. Rank-rank hypergeometric overlap: identification of statistically significant overlap between gene-expression signatures. Nucleic Acids Res. 2010;38:e169. https://doi.org/10.1093/nar/gkq636.
35. Ilg W, Müller B, Faber J, et al. Digital Gait Biomarkers Allow to Capture 1-Year Longitudinal Change in Spinocerebellar Ataxia Type 3. Mov Disord. 2022;37:2295–301. https://doi.org/10.1002/mds.29206.
36. Ilg W, Golla H, Thier P, Giese MA. Specific influences of cerebellar dysfunctions on gait. Brain. 2007;130:786–98. https://doi.org/10.1093/brain/awl376.
37. Lu J, Li D, Li F, et al. Montreal Cognitive Assessment in detecting cognitive impairment in Chinese elderly individuals: a population-based study. J Geriatr Psychiatry Neurol. 2011;24:184–90. https://doi.org/10.1177/0891988711422528.
38. Fabbri M, Del Campo N, Meissner WG, et al. Disease Progression in Multiple System Atrophy: The ASPIRE Multi-Modal Biomarker Study. Ann Neurol. 2026;99:96–113. https://doi.org/10.1002/ana.70028.

39. Gao M, Zhang H, Shan A, et al. Differences Between Patients With Multiple System Atrophy With Predominant Parkinsonism and Parkinson's Disease Based on fNIRS and Gait Analysis. CNS Neurosci Ther. 2025;31:e70342. https://doi.org/10.1111/cns.70342.
40. Mancini M, Afshari M, Almeida Q, et al. Digital gait biomarkers in Parkinson's disease: susceptibility/risk, progression, response to exercise, and prognosis. NPJ Parkinsons Dis. 2025;11:51. https://doi.org/10.1038/s41531-025-00897-1.

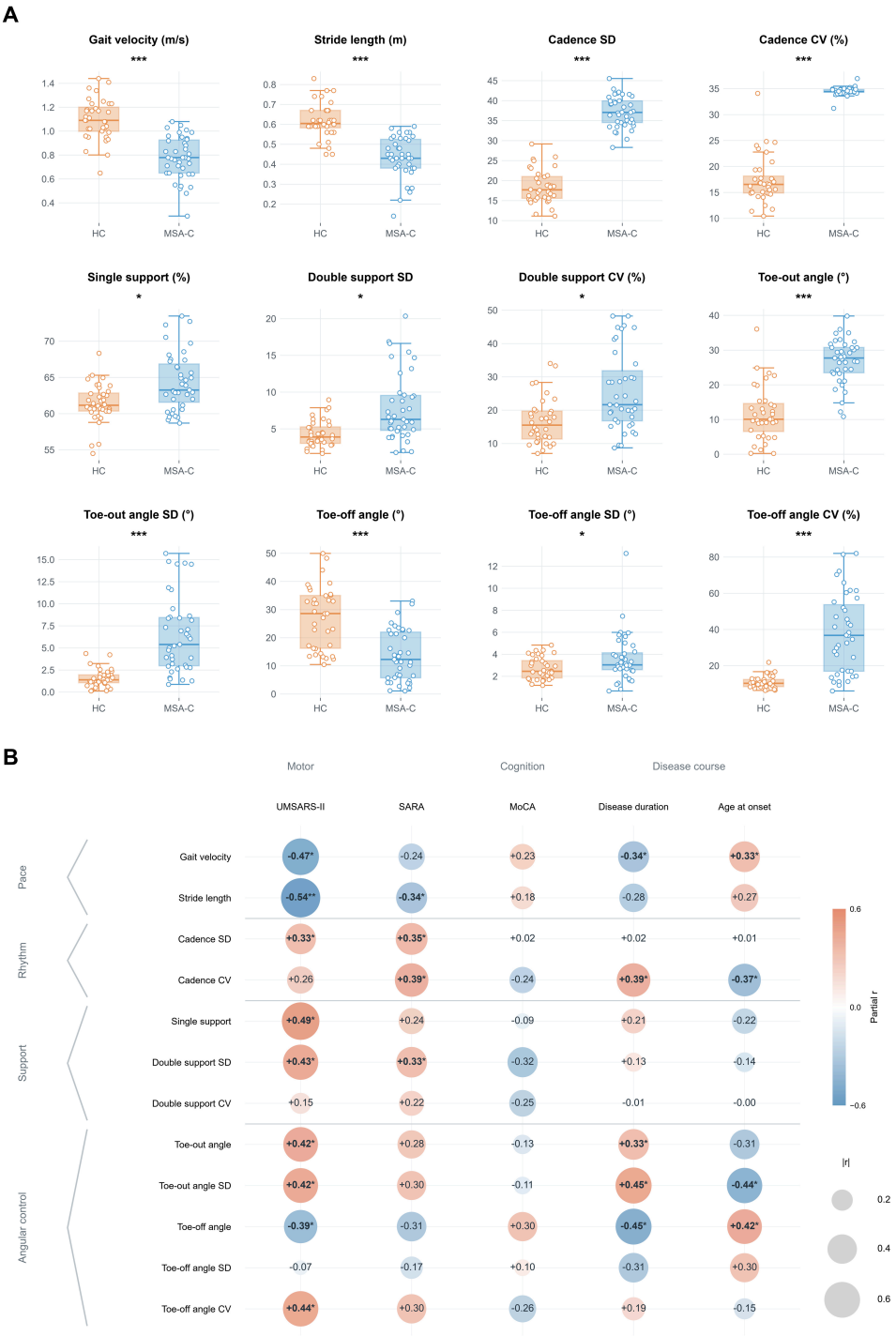
Table

Table 1. Baseline and clinical characteristics of the study participants

Variable	HC (n=36)	MSA-C (n=39)	Statistic / P value
Panel A. Baseline characteristics of healthy controls and patients with MSA-C			
Age, years	42.92 ± 15.37	56.41 ± 7.57	t=-4.76; P<0.001
Height, cm	165.22 ± 8.96	163.67 ± 7.56	t=0.81; P=0.418
Weight, kg	62.89 ± 10.66	64.00 ± 9.73	t=-0.47; P=0.638
Sex, n (%)			χ^2=0.00; P=0.955
Female	15 (41.67)	16 (41.03)	
Male	21 (58.33)	23 (58.97)	
Panel B. Clinical characteristics of patients with MSA-C			
Education, n (%)		MSA-C (n=39)	
Primary or less		23 (58.97)	
Junior secondary		9 (23.07)	
Senior secondary		6 (15.38)	
Junior college and undergraduate		1 (2.56)	
Disease duration, years (n=38)		2 (2, 3)	
Age at onset, years		53 (51, 58.5)	
SARA score		12.33 ± 3.92	
UMSARS total score		27.18 ± 8.80	
UMSARS-I score		12.95 ± 4.44	
UMSARS-II score		14 (10, 16)	
MMSE score		25 (22.5, 28)	
MoCA score		17.2 ± 6.51	

Note. Data are presented as mean ± standard deviation, median (Q1, Q3), or n (%), as appropriate. Abbreviations: HC, healthy controls; MSA-C, multiple system atrophy of the cerebellar type; SARA, Scale for the Assessment and Rating of Ataxia; UMSARS, Unified Multiple System Atrophy Rating Scale; MMSE, Mini-Mental State Examination; MoCA, Montreal Cognitive Assessment.

Figures



A: * q<0.05, ** q<0.001, *** q<0.0001 (BH-FDR across 20 age-adjusted group tests).

B: * P<0.05, ** P<0.001 (nominal two-sided); age and sex adjusted; n=39.

Figure 1

Gait abnormalities and clinical associations in MSA-C. (A) Raw distributions of the 12 gait features that differed between groups after age-adjusted testing of all 20 features and BH-FDR correction across the 20 comparisons; *q<0.05, **q<0.001, and ***q<0.0001. (B) Age- and sex-adjusted partial-correlation matrix relating the 12 abnormal gait features to UMSARS-II, SARA, MoCA, disease duration, and age at onset. In panel B, *P<0.05 and **P<0.001 indicate nominal two-sided significance; no multiplicity

correction was applied to these clinical-gait correlations. Detailed numerical results are provided in Supplementary Tables S1-S2.

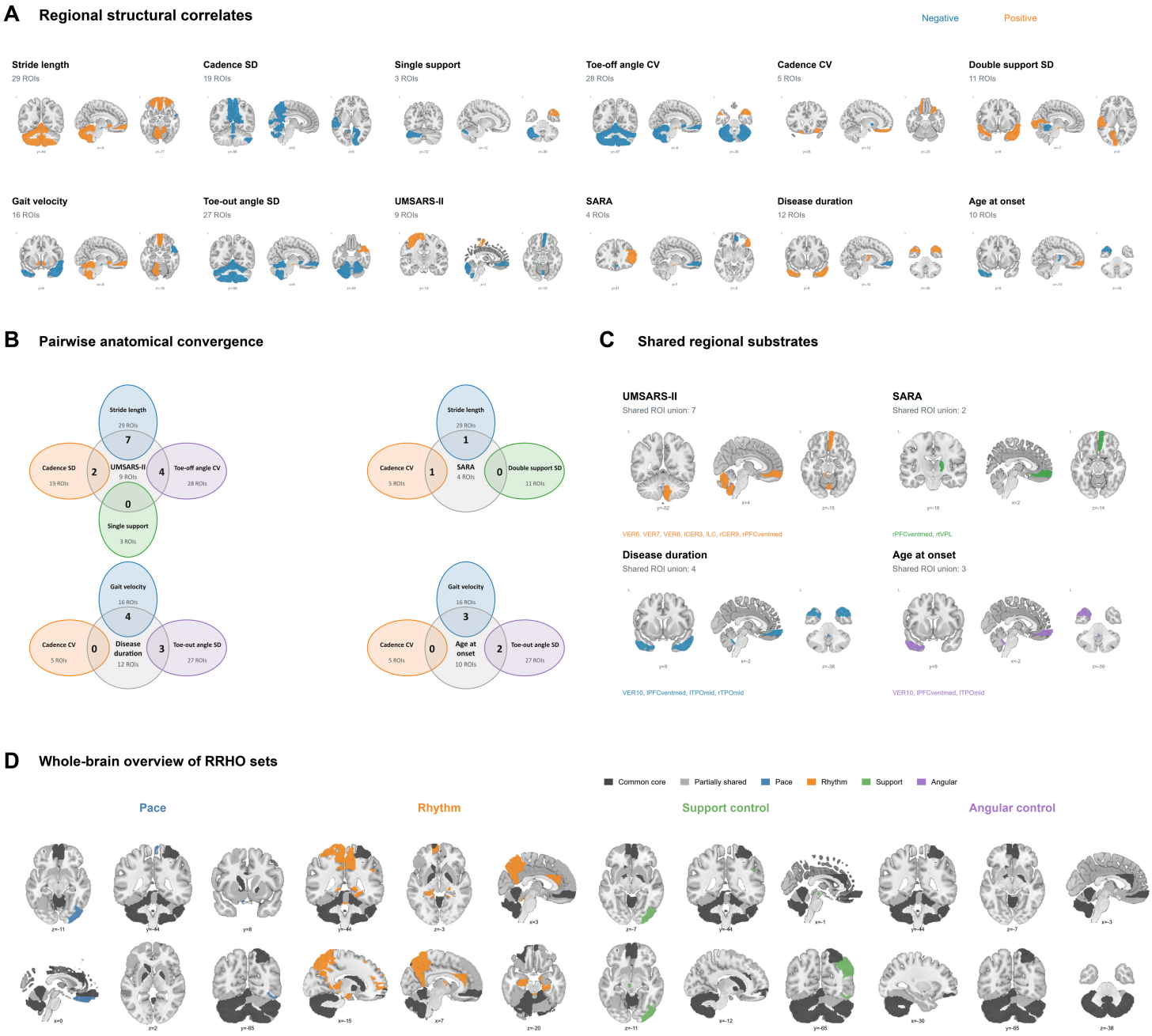


Figure 2

Shared gray-matter correlates of gait and clinical phenotypes in MSA-C. (A) Regional GMV associations for representative gait features and clinical phenotypes (nominal two-sided P<0.05); color indicates correlation direction. (B) Pairwise overlap; numbers indicate ROI counts in each map and their intersection. (C) Union of shared ROIs across gait features for each phenotype. (D) Spatial similarity of directionally harmonized 163-ROI effect maps (Spearman r_map); * indicates nominal two-sided P<0.05 from 10,000 subject-level residual permutations. Exact P values are in Supplementary Table S7. (E) Rank-

rank hypergeometric overlap (RRHO) by gait domain; dark gray denotes common-core ROIs, light gray partial overlap, and colors the gait domains. Details are in Supplementary Methods S5 and Tables S4–S10.

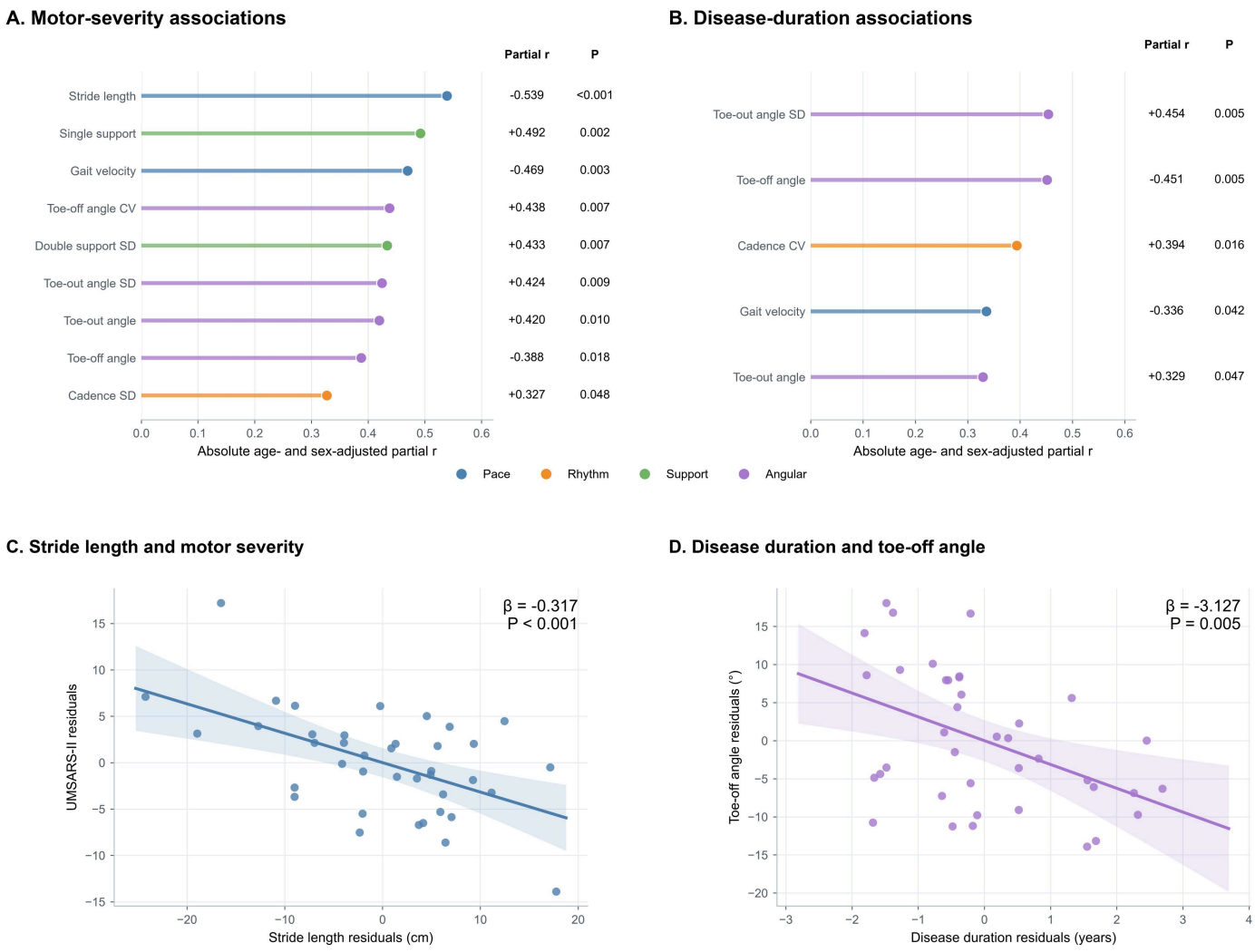


Figure 3

Prioritization and clinical interpretation of gait markers for motor severity and disease duration. (A-B) Relative cross-validated performance and bootstrap ranking stability of candidate gait markers for UMSARS-II and disease duration. (C) Age- and sex-adjusted association between stride length and UMSARS-II. (D) Age- and sex-adjusted association between disease duration and toe-off angle. Detailed results are provided in Supplementary Tables S11-S12.

Supplementary Files

This is a list of supplementary files associated with this preprint. Click to download.

- MSACSupplementaryMaterialsFig2Dtwosided.docx